Liquid Xenon Positron Target

Max Varverakis* and Robert Holtzapple†
California Polytechnic State University, San Luis Obispo, CA 93407, USA

Spencer Gessner‡
SLAC National Accelerator Laboratory, Menlo Park, California 94025, USA

Hiroki Fujii§
Nishina Center, RIKEN, 2-1 Hirosawa, Wako, Saitama, 351-0198, Japan
(Dated: November 23, 2022)

Positron targets are a critical component of future linear colliders. Traditional targets are composed of high-Z metals that become brittle over time due to constant bombardment by high-power electron beams. We explore the possibility of a liquid Xenon target which is constantly refreshed and therefore not susceptible to the damage mechanisms of traditional solid targets. Using GEANT4 simulation code, we examine the performance of the liquid Xenon target and show that the positron yield and divergence are comparable to solid targets when normalizing by radiation length. Additionally, we observe that the peak energy deposit density (PEDD) threshold for LXe is higher than for common solid targets, which makes it an attractive positron target alternative. We develop parameter sets for a demonstration application at FACET-II, ILC, C^3, and at an ideal linear accelerator designed around the LXe target.

I. INTRODUCTION

Future linear colliders require approximately 10^{14} e^+ per second at the IP in order to achieve luminosities in excess of 10^{34} $\mathrm{cm}^{-2}\mathrm{s}^{-1}$ [1]. Traditionally, positrons are produced by colliding high energy electrons into a high-Z solid target, where positrons are created from the resulting electromagnetic shower. In order to generate 10^{14} e^+ per second, an extremely high-power electron beam is required, which results in large power deposits in the target that degrades high-Z solid targets over time [2].

Previous experiments have explored alternatives to solid targets. Several of studies investigated using liquid Mercury (Hg), but the apparent hazards that Hg presents limits its applications [3]. Additional liquid targets that have been examined in the undulator scheme for ILC include Pb [4] and Bi-Pb [3]. Liquid targets have been studied for other particle type generators such as using liquid Lithium to generate neutrons from a proton beam [5] and a gaseous deuterium target and proton beam for muon production [6]. Mention LEMMA? ([7])

Xenon is a nonreactive high-Z substance that can be converted into a dense liquid at relatively high temperatures. Consequently, liquid xenon (LXe) has several useful properties in regard to positron production: 1) LXe has a relatively short radiation length for a nonmetal; 2) LXe has a high PEDD threshold compared to typical solid target materials because of its large heat of vaporization. This allows vaporized Xe to be refreshed by LXe through a flow mechanism of the target; and 3) Using LXe as a positron target removes the concern of long term degradation observed with solid positron targets. The above factors make LXe a promising candidate for a positron target.

In this paper, we explore the use of a LXe positron target with the necessary flow rate to adequately handle the power deposited by a high power electron beam.

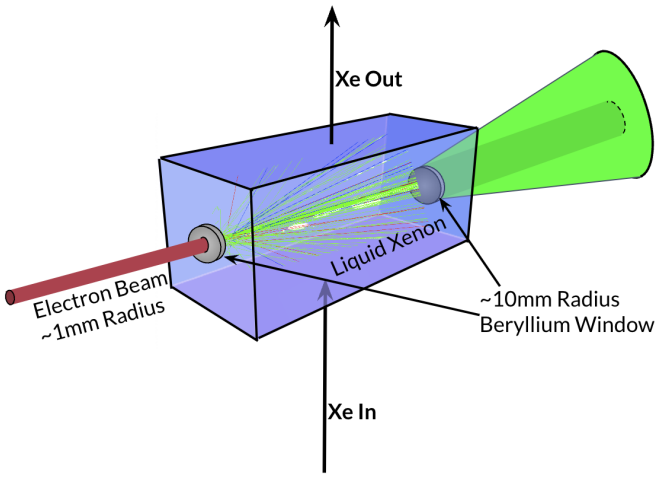

FIG. 1. The liquid Xenon target setup. A 10 GeV electron beam is incident on the target from the left. The beam enters and exits the LXe target through a 10 mm diameter, 0.5 cm-thick Be window. The positrons exit the target and travel to the right. Fresh LXe is pumped vertically through the target chamber to replace the heated LXe.

II. SIMULATION RESULTS

Figure 1 illustrates the LXe target-beam interaction simulated using GEANT4 [8] G4EMStandardPhysics

* mvarvera@calpoly.edu
† rholtzap@calpoly.edu
‡ sgess@slac.stanford.edu
§ hiroki.fujii@riken.jp

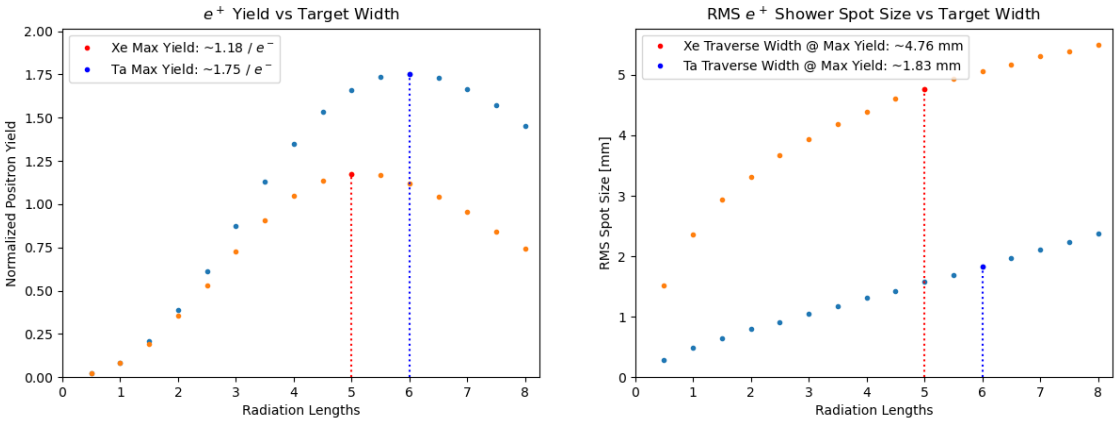

FIG. 2. Positron yield and RMS transverse displacement upon exiting the target per incident e^- at 10 GeV.

package to quantify positron production/beam parameters from the electromagnetic shower for both the LXe and Tantalum targets. Previous studies at FACET-II considered a solid Tantalum (Ta) target, rather than the traditional tungsten (W) target, for positron generation [9] which will serve as a useful comparison to the results of the LXe target.

Although tungsten (W) alloys are commonly used materials for conventional positron targets,we expect similar results for different solid target materials when normalizing by radiation lengths and therefore use Ta as a comparison.

The figures of merit used to compare the two targets are: 1) positron yield; 2) RMS spot size; and 3)energy deposition at the target. For these comparisons, we only consider positrons at the exit of the target with an energy range of 2 MeV to 60 MeV and under 10 mm transverse displacement, which is based off of similar positron acceptances in [10, 11]. Note that these cutoffs are for positrons just after exiting the target rather than at the end of a capture section of the accelerator.

The figures are out of order numerically. Table I shows the parameters used in the GEANT4 simulations.

Material	**Z**	**Density** [g · cm^{-3}]	**Rad Length** [cm]
Tantalum (Ta)	73	16.654	0.4094
Liquid Xe (LXe)	54	2.953	2.872

TABLE I. Parameters used in GEANT4 simulation when comparing targets.

Figure 2 displays positron yield and spot size as a function of radiation length for Ta and LXe. next sentence may change Although Figure 2 indicates that the maximum positron yield occurs at a smaller radiation length for LXe compared to Ta, the radiation length corresponding to maximum positron yield would be the same for both targets if we remove the energy and spot size cutoffs. Observe that both targets generate a similar yield distribution when normalizing by radiation lengths, as predicted. The energy spectrum of the positrons exiting the target are relatively equal for both target materials despite having different radiation lengths.

At maximum positron yield, the transverse emittance for Ta is 14mm · rad while the transverse emittance for LXe is 33mm · rad. Even with a larger transverse emittance, the LXe emmittance is consistent with proposals at CLIC, NLC, and ILC [1, 10, 12]. Ignoring our cuts in the data, the emittance and spot size for LXe is roughly 5 times larger than Ta, which can be attributed to their difference in radiation lengths. Despite both having the same angular divergence, the difference in radiation lengths is great enough that we find a larger RMS spot size for LXe compared to Ta in Figure 2 even with our cuts in place.

We extract energy deposited in the target from the simulations which is a critical component of our flow calculations in the following section. Figure 3 compares the energy deposited in the target for each material per incident e^-. As we indicate in Section III A, the flow of LXe accounts for the energy deposit. It is clear from Figure 3 that both targets follow the same energy deposition distribution as a function of radiation length.

Parameter	Unit	FACET-II [13]	ILC [14]	C^3 [15]	Optimal
Energy	GeV	10	3	3	10
e^-/bunch	10^{10}	1.25	2.5	0.78	1.125
Bunches/train		1	1312	133	1000
Rep. rate	Hz	10	5	120	11.10
PEDD/train	J · g^{-1}	0.107	84.0	2.66	96.1
Flow rate	L · s^{-1}	0.0049	0.073	1.75	0.16
Beryllium Window					
E_{dep}/bunch train	J	0.014	10.65	0.34	12.18
Temperature change	K·s^{-1}	2.56	1009	766	2560

TABLE II. Electron beam parameters and associated target quantities for FACET-II, ILC, C^3, and the optimal beam setup. The Beryllium window quantities are specific to a 10mm radius, 0.5 mm-thick Be disk. Note that the window parameters correspond to the exit window only since the entrance window receives a significantly smaller energy deposit per incident e^-.

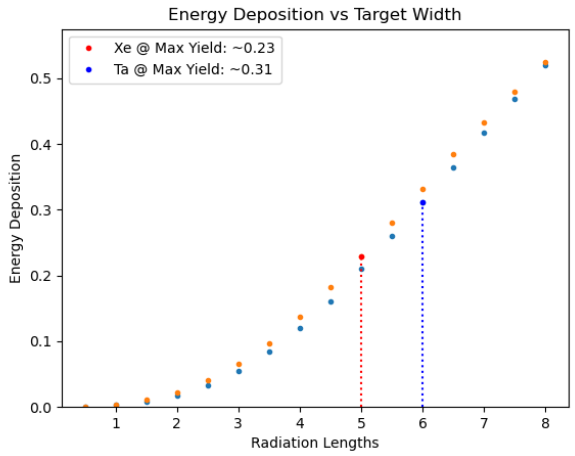

FIG. 3. RMS fractional energy deposition in Ta and LXe targets per incident electron at 10 GeV.

III. ENERGY DEPOSITIONS AND FLOW CONSIDERATIONS FOR LXE

A. Calculating the LXe Flow Rate

For our calculations, we assumed a spot size of 6 mm radius which was determined by the shower size. This resulted in a volume of 14.6 cm^3 of LXe interacting with the beam shower. By using heat of vaporization, we determined the energy required to vaporize the LXe. PEDD is calculated by considering the energy deposit per bunch train and the mass of the interacting volume of LXe (43.16 g). Note that some of the PEDD values in Table II far exceed the typical maximum PEDD of 35 J · g^{-1} for solid targets [1]. Since the LXe is constantly circulating in the target, the PEDD is not a limiting factor for the LXe target. By using the bunch train energy deposits and beam repetition rates along with the amount of energy required to vaporize LXe for a given volume (calculated to be 284.205 J·cm^{-3}), the time required to vaporize the 14.6 cm^3 of LXe was obtained. We based the LXe flow rates off of the time evacuate the volume before the next bunch train arrival at the target. Subject to change.

When considering the optimal beam parameters for the LXe target, we assumed a delivery rate of 10^{14} $e^+ \cdot \text{s}^{-1}$ to the IP. We also assumed a safety factor of 1.5 positrons after the target which gave a positron yield of 1.2 per incident electron. Lastly, we took the drive bunch energy to be 10 GeV and the energy deposition to be 2.3 GeV/e^-, which was based off of the simulation results. From these assumptions, we chose the beam parameters that brought the energy deposit per bunch train closest to the energy required to vaporize the LXe.

B. Beryllium Windows for the Target Chamber

We explore using Beryllium (Be) windows for the beam to enter and exit the target chamber. The pressure on the Be windows is dominated by the vapor pressure of LXe which is around 300 kPa. Reference [16] provides a method to calculate the required thickness of the Be windows, which we found to be 0.5 mm. Using this thickness, we simulated the energy deposited in the Be windows and found that the energy deposited in the entrance window is on the order of 10^{-1} MeV/incident e^- and the exit window on the order of 6 MeV/incident e^-. According to the conclusions of [17], the temperature shocks corresponding to the energy deposits in the windows is of negligible concern at FACET-II. However, we would expect to see microcracks in the exit window for ILC and C^3. Note that the melting point of Beryllium is 1285 °C, so the temperature change corresponding to the optimal beam parameters requires attention.

IV. CONCLUSION

Through GEANT4 simulations, we determined that a LXe e^+ target produces comparable yields to its solid target counterparts. The benefit of using a LXe target is that it does not deteriorate over time as compared to solid

targets which require replacement due to degradation. Despite the slight discrepancies in e^+ spread between solid targets and LXe, the apparent benefits of using a LXe target outweighs this disadvantage. The most important considerations while building a LXe apparatus would be accounting for the pressure of the Xenon and the corresponding flow rates. Using Be windows for the beam entrance and exit of the LXe target chamber have minimal affect on the beam quality output according to simulations, and should be considered for use when designing a LXe target. Note that for certain beam parameters the Be windows may not be well-suited for the high temperature changes. In such cases, additional considerations should be made for the target windows. Further exploration of LXe positron target could entail more detailed simulations of the beam interaction with the LXe, such as cavitation bubbles and turbulent flows, as well as simulating a capture system on the exit of the target. It may also be useful to determine the energy deposit in the LXe as a function of target depth to better approximate flow rates. Source code and sample data from GEANT4 simulations can be found at `https://github.com/MaxVarverakis/LiquidXenonSims.git`.

[1] Y. Seimiya, M. Kuriki, T. Takahashi, T. Omori, T. Okugi, M. Satoh, J. Urakawa, and S. Kashiwagi, Progress of Theoretical and Experimental Physics **2015**, 103G01 (2015).

[2] V. Bharadwaj, Y. Batygin, J. Sheppard, D. Schultz, S. Bodenstein, J. Gallegos, R. Gonzales, J. Ledbetter, M. Lopez, R. Romero, T. Romero, R. Rutherford, and S. Maloy, in PACS2001. Proceedings of the 2001 Particle Accelerator Conference (Cat. No.01CH37268), Vol. 3 (2001) pp. 2123–2125 vol.3.

[3] A. A. Mikhailichenko, in Proceedings of EPAC 2006, Edinburgh, Scotland (2006).

[4] J. C. Sheppard, Liquid metal target for NLC positron source (2002).

[5] G. Feinberg, M. Paul, A. Arenshtam, D. Berkovits, Y. Eisen, M. Friedman, S. Halfon, D. Kijel, A. Nagler, A. Shor, and I. Silverman, in Proceedings of 11th Symposium on Nuclei in the Cosmos — PoS(NIC XI) (Sissa Medialab, 2011).

[6] H. Okita, Y. Ishi, and Y. Mori, Nuclear Instruments and Methods in Physics Research Section A: Accelerators, Spectrometers, Detectors and Associated Equipment **982**, 164565 (2020).

[7] D. Alesini, M. Antonelli, M. E. Biagini, M. Boscolo, O. R. Blanco-García, A. Ciarma, R. Cimino, M. Iafrati, A. Giribono, S. Guiducci, L. Pellegrino, M. Rotondo, C. Vaccarezza, A. Variola, A. Allegrucci, F. Anulli, M. Bauce, F. Collamati, G. Cavoto, G. Cesarini, F. Iacoangeli, R. L. Voti, A. Bacci, I. Drebot, P. Raimondi, S. Liuzzo, I. Chaikovska, R. Chehab, N. Amapane, N. Bartosik, C. Biino, A. Cappati, G. Cotto, N. Pastrone, M. Pelliccioni, O. S. Planell, M. Casarza, E. Vallazza, G. Ballerini, C. Brizzolari, V. Mascagna, M. Prest, M. S. A. Bertolin, C. Curatolo, F. Gonella, A. Lorenzon, D. Lucchesi, M. Morandin, J. Pazzini, R. Rossin, L. Sestini, S. Ventura, M. Zanetti, F. Carra, P. Sievers, L. Keller, L. Peroni, and M. Scapin, Positron driven muon source for a muon collider (2019).

[8] S. Agostinelli et al. (GEANT4), Nucl. Instrum. Meth. A **506**, 250 (2003).

[9] H. Fujii, K. Marsh, W. An, S. Corde, M. Hogan, V. Yakimenko, and C. Joshi, Physical Review Accelerators and Beams **22**, 10.1103/physrevaccelbeams.22.091301 (2019).

[10] H. Tang, A. Kulikov, J. Clendenin, S. Ecklund, R. Miller, and A. Yeremian, in Proceedings Particle Accelerator Conference (IEEE, 1995).

[11] J. Sheppard, Conventional positron target for a tesla formatted beam(LCC-0133) (2003).

[12] A. Vivoli, I. Chaikovska, R. Chehab, O. Dadoun, P. Lepercq, F. Poirier, L. Rinolfi, V. Strakhovenko, and A. Variola, The CLIC Positron Capture and Acceleration in the Injector Linac., Tech. Rep. (CERN, Geneva, 2010).

[13] N. G. Author, Technical design report for the FACET-II project at SLAC national accelerator laboratory (2016).

[14] H. Nagoshi, M. Kuribayashi, M. Kuriki, P. Martyshkin, T. Omori, T. Takahashi, M. Yamakata, and K. Yokoya, Nuclear Instruments and Methods in Physics Research Section A: Accelerators, Spectrometers, Detectors and Associated Equipment **953**, 163134 (2020).

[15] M. Bai, T. Barklow, R. Bartoldus, M. Breidenbach, P. Grenier, Z. Huang, M. Kagan, J. Lewellen, Z. Li, T. W. Markiewicz, E. A. Nanni, M. Nasr, C.-K. Ng, M. Oriunno, M. E. Peskin, T. G. Rizzo, J. Rosenzweig, A. G. Schwartzman, V. Shiltsev, E. Simakov, B. Spataro, D. Su, S. Tantawi, C. Vernieri, G. White, and C. C. Young, C^3: A "cool" route to the higgs boson and beyond (2021).

[16] Crystran Ltd, The CRYSTRAN HANDBOOK of Infra-Red and Ultr (2019).

[17] K. Ammigan, S. Bidhar, P. Hurh, R. Zwaska, M. Butcher, M. Calviani, M. Guinchard, R. Losito, V. Kuksenko, S. Roberts, A. Atherton, G. Burton, O. Caretta, T. Davenne, C. Densham, M. Fitton, P. Loveridge, and J. O'Dell, Physical Review Accelerators and Beams **22**, 10.1103/physrevaccelbeams.22.044501 (2019).